International Journal of Civil Engineering (2024) 22:2407–2419
https://doi.org/10.1007/s40999-024-01009-5

RESEARCH PAPER

Characterization of Limestone Calcined Clay Cement Made with Calcium Sulfoaluminate Clinker

Muhammet Atasever[1] · Sinan Turhan Erdoğan[2]

Received: 31 December 2023 / Revised: 4 June 2024 / Accepted: 17 June 2024 / Published online: 2 July 2024

Abstract

This study concentrated on producing limestone calcined clay calcium sulfoaluminate cement by replacing portland cement in limestone calcined clay cement with calcium sulfoaluminate cement, with the goal of increasing the early strength of limestone calcined clay cement. The mineralogy and microstructures of hydrating pastes were investigated using x-ray diffraction and scanning electron microscopy. Heat evolution was studied using isothermal calorimetry. Strength development and workability were assessed on mortar samples. The 1 day strengths of limestone calcined clay calcium sulfoaluminate cement samples exceeded those of limestone calcined clay cement by ∼ 30–80%, though its strength gain slows significantly after 1 day due to the lack of calcium silicates, affecting pH and clay dissolution. Despite this, the strength development of limestone calcined clay calcium sulfoaluminate cement, when adjusted for CO_2 emissions, is comparable to limestone calcined clay cement. Additionally, limestone calcined clay calcium sulfoaluminate cement provides a 10–15% higher flow and exhibits a lower heat of hydration beyond 12 h, while maintaining a production cost similar to that of limestone calcined clay cement.

Keywords Calcium sulfoaluminate · Calcined clay · Limestone · Cement · Strength

1 Introduction

Ambitious goals set to drastically reduce CO_2 emissions and eventually achieve net zero [1, 2] have prompted the construction industry to accelerate research on developing low-carbon alternatives to portland cement (PC). The main sources of CO_2 emissions in PC production are the decarbonation of limestone, the combustion of fuel to heat the kiln to ∼ 1500 °C, and the grinding of clinker. While PC possesses remarkable technical properties, its production releases ∼ 0.9 tons of CO_2 for every ton of PC produced [3]. With nearly ∼ 4.1 billion tons of PC produced annually [4], attempts have been made to develop cements with reduced PC clinker content. Pozzolan-blended cements are notable examples that can exhibit properties similar to, or even surpass, those of traditional PC mixtures. However, substituting PC clinker with pozzolan invariably results in reduced strength at early ages, particularly when high replacement ratios are utilized [5–7]. Limestone calcined clay cement (LC^3), based on the synergy between limestone, calcined clay, and PC clinker, offers a partial solution to this issue of compromised early-age strength. Additional hydration products, predominantly carboaluminates and ettringite, accelerate the development of strength [8]. As a result, LC^3 formulations using metakaolin or kaolinite-rich clays, have demonstrated the ability to match the strength of PC-only mixtures, as early as 3 days [9]. Nonetheless, typical LC^3, containing ∼ 50% PC clinker, has low strength up to 3–7 days. A potential solution might be the substitution of PC clinker with the more rapidly reacting calcium sulfoaluminate cement ($C\overline{S}A$) clinker. $C\overline{S}A$ is a low-carbon alternative cement, offering 25–35% lower emissions than PC [10]. However, its production involves the use of limestone, gypsum, and bauxite. The incorporation of bauxite, utilized as an

✉ Sinan Turhan Erdoğan
sinante@metu.edu.tr

Muhammet Atasever
muhammet.atasever@agu.edu.tr; mataseve@metu.edu.tr

[1] Department of Civil Engineering, Abdullah Gül University, Kayseri, Turkey

[2] Department of Civil Engineering, Middle East Technical University, Ankara, Turkey

alumina source to form ye'elimite ($C_4A_3\overline{S}$), the primary clinker phase in $C\overline{S}A$ clinker, results in a higher cost compared to PC clinker [10–12]. The combination of LC^3 and $C\overline{S}A$ may offer an optimal balance between cost-effectiveness and early-age strength. The use of mineral admixtures in $C\overline{S}A$ cement to reduce cost is already common practice [13–19]. A study into the effects of metakaolin and calcined montmorillonite on $C\overline{S}A$ revealed that both replacements up to 20% led to reduced strength and heat evolution without the formation of new hydration products [20]. In another study, ground granulated blast furnace slag (GGBFS), which has a lower aluminate content than kaolinitic clay decreased both the rate of heat evolution and total hydration heat despite having no significant impact on the formation of hydration products. Nonetheless, the compressive strength of mortars containing 10% or less GGBFS remained comparable to that of mortars without GGBFS but not at early ages [21]. The positive effects of limestone or dolomite powder on the strength of $C\overline{S}A$ cement have also been reported [22]. Fewer studies have been conducted on the impact of both kaolinite clay and limestone on $C\overline{S}A$ cement performance. One such study investigated the hydrate phase assemblage of $C\overline{S}A$ cement blended with metakaolin and limestone and found that while ye'elimite achieved full hydration by 91 days, belite did not. The primary hydration products identified were stratlingite, hemicarbonate, C–S–H, $Al(OH)_3$, and ettringite [23]. The presence of limestone stabilized ettringite but the faster reaction of metakaolin compared to belite resulted in the release of less calcium to drive the pozzolanic reactions. However, strength development was not reported. Another investigation used a binder that could be considered similar to LC^3 made with $C\overline{S}A$, partially replacing increasing amounts of portland limestone cement (PLC) with a belitic $C\overline{S}A$ and a calcined clay [24]. The strength of a mortar made with 30% PLC + 40% $C\overline{S}A$ + 30% calcined clay reached 12 MPa at 1 d. Higher levels of $C\overline{S}A$ further increased early strength but greatly reduced strength gain beyond 1 day. There is a scarcity of experimental studies that investigate the combined effect of clay and limestone on $C\overline{S}A$. Also, the nature of the clay and $C\overline{S}A$ clinker used can lead to drastically different hydrated microstructures in such systems. The present study investigates the effect of replacing the PC clinker component in LC^3 with $C\overline{S}A$ clinker to formulate a binder that has higher early-age strength than typical LC^3 and lower cost than $C\overline{S}A$, while still maintaining the environmental advantage of having a reduced clinker content. Such a binder could not only be preferable environmentally to traditional PC but preferable technically to typical LC^3 for use in applications where early strength gain can be important, such as low-temperature applications.

2 Materials and Experimental Methods

2.1 Materials

The LC^3 blends in this study were prepared in the laboratory by combining a PC clinker (Baştaş Cement Plant, Ankara), limestone and gypsum (Votorantim Hasanoğlan Cement Plant, Ankara), and kaolinitic clay from Balıkesir (used after calcining). The $C\overline{S}A$ clinker was also prepared in the laboratory, using the same limestone and gypsum as well as bauxite (Seydişehir Eti Aluminum Plant, Konya).

Table 1 Oxide composition and physical properties of materials used

Oxide (%)	PC clinker	$C\overline{S}A$ clinker	Kaolinitic clay	Gypsum	Limestone	Bauxite
CaO	69.9	52.7	0.2	37.3	53.5	1.1
SiO_2	18.3	10.5	55.2	0.6	1.1	11.7
Al_2O_3	4.1	13.2	30.1	0.2	0.4	49.6
Fe_2O_3	3.4	12.3	0.7	0.1	0.2	16.9
MgO	1.4	0.7	0.1	0.2	0.4	0.3
K_2O	1.3	0.3	0.8	0.0	0.1	0.3
SO_3	1.0	10.3	2.9	47.0	0.1	0.4
Na_2O	0.4	–	–	–	–	–
Loss on ignition	0.1	4.1	10	14.6	44.2	19.8
Density (g/cm^3)	3.16	3.00	2.63	2.51	2.72	3.15
Blaine Fineness (cm^2/g)	3700	4000	10,000	3500/8000*	10,000	N/A**

*3500 cm^2/g for LC^3 and 8000 cm^2/g for $C\overline{S}A$ clinker and cement

**Bauxite was only used in the kiln feed to prepare $C\overline{S}A$. It was not used as an added agent in the prepared mixtures

The chemical compositions of the raw materials, determined using X-ray fluorescence spectroscopy (XRF), and some physical properties are provided in Table 1.

All ingredients were ground using a ball mill. Although the clinkers have similar fineness, the clay and limestone are finer. The clay contains ~ 85% by mass $SiO_2 + Al_2O_3$, and has a loss on ignition value of 10%, meeting ASTM C 618 [25]. The PC clinker is of the CEM I type with rather high alkali and low aluminate content. The bauxite used to produce $C\overline{S}A$ clinker is borderline low grade, with < 50% low Al_2O_3. Hence the $C\overline{S}A$ clinker contains less aluminium than many commercial ones. 40% limestone (for CaO), 40% bauxite (for Al_2O_3), and 20% gypsum (for SO_3) were calcined at 1300 °C for 120 min in an electric furnace (Protherm MoS-B 160/8) as detailed in [12]. Figure 1a shows the X-ray diffraction (XRD) pattern for this $C\overline{S}A$ clinker. Quantitative analysis with Rietveld refinement suggests this clinker is made up of ye'elimite (28.2%), brownmillerite (34.3%), and belite (37.5%) with an agreement factor, R_{wp} = 8.8%. As expected due to the use of a low-grade, more economical bauxite, it has a ye'elimite-to-belite ratio less than 1, lower than most commercial $C\overline{S}A$ clinkers. As this ratio increases, the contribution to early strength but also the production cost of the $C\overline{S}A$ could be expected to increase. Figure 1b shows that the PC clinker contains C_3S (68.4%), C_2S (21.8%), C_3A (4.1%), and C_4AF (5.7%) with R_{wp} = 14.6%.

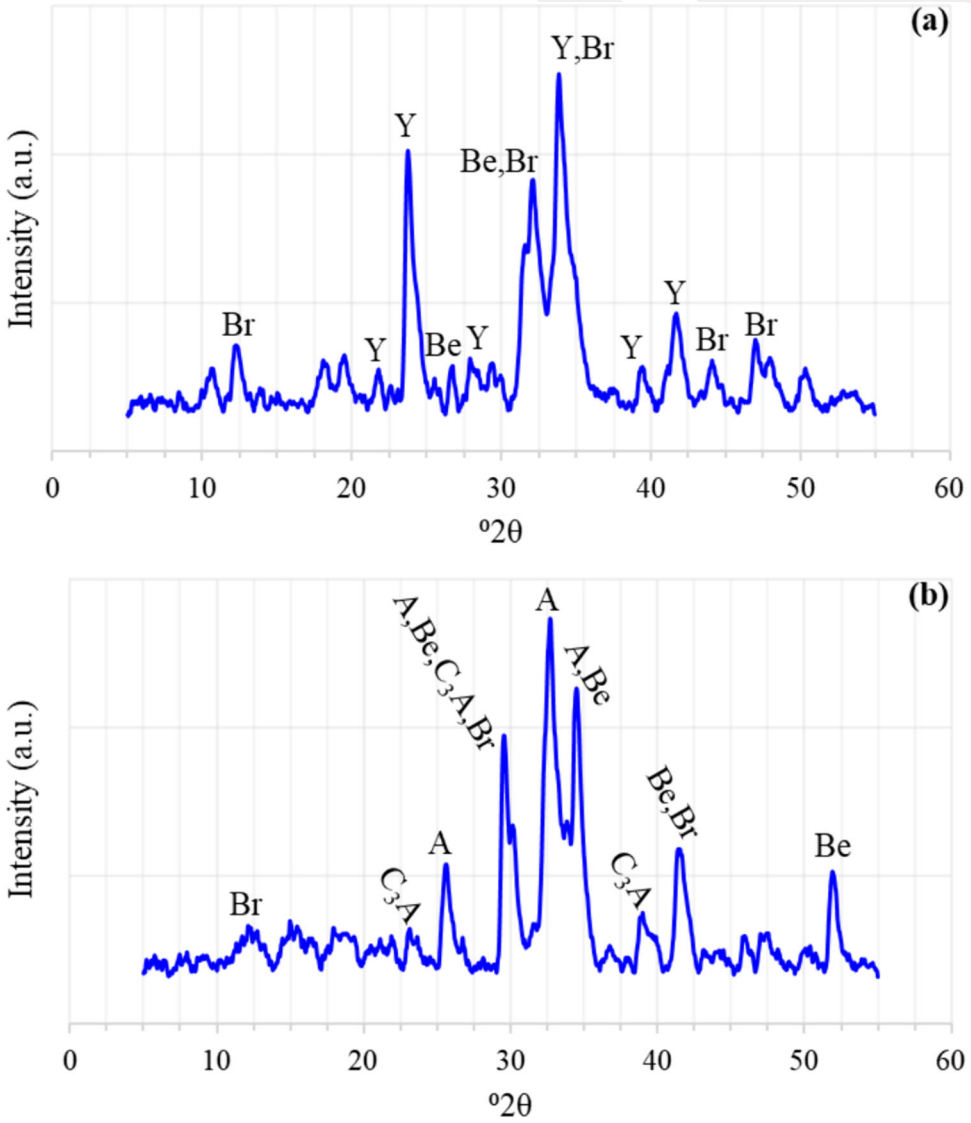

Fig. 1 X-ray diffractograms for (a) $C\overline{S}A$ clinker (b) PC clinker (Legend: Be-Belite; Br-Brownmillerite; C_3A-Tricalcium aluminate; A-Alite; Y-Ye'elimite)

Table 2 Binder proportions for the various mixtures studied (wt. %)

Cement ID	$C\bar{S}A$ clinker	PC clinker	Calcined clay	Limestone	Gypsum
PC-Control	–	94.0	–	–	6.0
$C\bar{S}A$ -Control	81.0	–	–	–	19.0
PC-LC^3-52	–	51.7	30.0	15.0	3.3
$C\bar{S}A$ -LC^3-57	56.7	–	20.0	10.0	13.3
$C\bar{S}A$ -LC^3-51	50.6	–	25.0	12.5	11.9
$C\bar{S}A$ -LC^3-45	44.6	–	30.0	15.0	10.5

3 Mixture Design

Table 2 presents the studied paste and mortar mixtures. Gypsum:clinker was chosen as 6:94 for PC-Control according to ASTM C563 [26] while the same ratio was 19:81 for $C\bar{S}A$ -Control, previously determined as the optimum ratio for the particular $C\bar{S}A$ clinker produced here [12].

PC-LC^3-52 represents a "typical" LC^3 based on studies in the literature [27–30]. PC clinker makes up roughly half of the LC^3 while the ratio of clay-to-limestone is 2 [5, 31–34]. Three different $C\bar{S}A$ clinker contents were chosen for the $C\bar{S}A$ -LC^3 mixtures, one similar to that of PC-LC^3-52, one slightly higher, and one slightly lower. The clay-to-limestone ratio is kept as 2 but the gypsum content is higher than in PC-LC^3-52 due to the need for sulfates in the hydration of $C\bar{S}A$ (to form ettringite from ye'elimite). All three $C\bar{S}A$ -LC^3 blends have been designed to be lower carbon than PC-Control and $C\bar{S}A$ -Control because of their lower clinker contents and lower carbon than PC-LC^3-52 because $C\bar{S}A$ is lower carbon than PC (Fig. 2). The suitable calcination temperature for the clay was determined by comparing the strength activity indices (ASTM C618 [25]) of mortars prepared using PC and the clay calcined at 600, 650, 700, 750, and 800 °C were compared. The highest activity was obtained using clay calcined at 650 °C, consistent with the literature for kaolinitic clays [5, 34–38].

The calculations made for Fig. 2 are based on data related with the production of PC [39] and the production of $C\bar{S}A$ [10]. The entire clinker production process is considered, including raw meal preparation (quarrying, crushing, and initial grinding), production/kiln consumption system (fuel burning and chemical reaction), and finishing (milling, blending, mixing, and transportation). CO_2 emitted per ton of PC-Control (100% in Fig. 2) is ~ 1.08 t of CO_2 while the total CO_2 produced for $C\bar{S}A$ -Control throughout all processes is calculated to be ~ 0.62 t. Emissions related to the production of limestone and calcined clay were examined separately. CO_2 emissions due to the quarrying and crushing of limestone and calcined clay were assumed to be the same as that of PC clinker. However, CO_2 emissions due to the grinding of limestone were calculated using grindability (energy expenditure required for grinding) vs. Blaine specific surface area data in [35]. CO_2 emission data related to the production of calcined clay was taken from [40] and finally, the emissions related

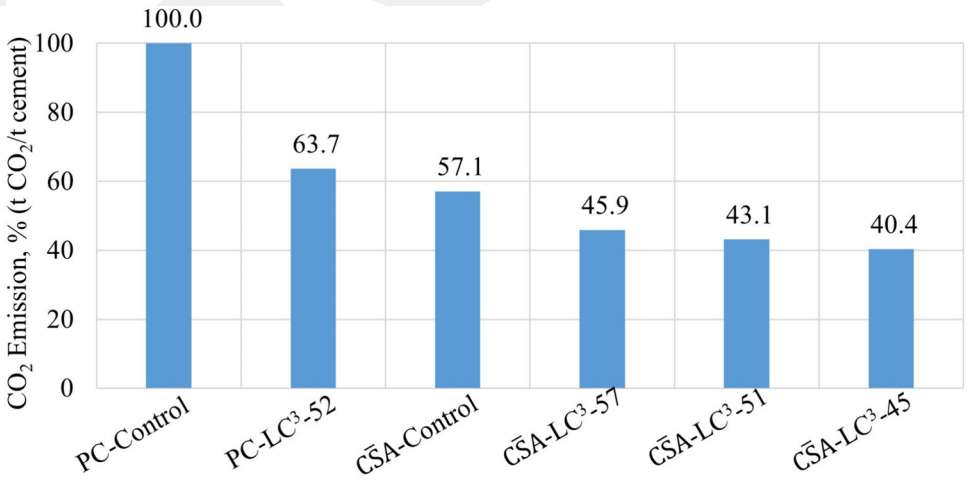

Fig. 2 Comparison of CO_2 emission during the production of the various binders (adapted from [10, 35, 39, 40])

to the production stages of $C\bar{S}A$ cement were calculated using data in [10].

4 Test methods

Mortars with water-to-binder ratio (W/B) of 0.50 were prepared using silica sand in a laboratory mixer according to ASTM C305 [41] for evaluation of strength development up to 28 days, and cast in 50 mm cube molds as per ASTM C109 [42]. The fresh properties of mortars were assessed using a flow table, according to ASTM C1437 [43]. Water-cured $C\bar{S}A$ cement samples reportedly have lower AFt/AFm, resulting in lower strength compared to air-cured samples [44]. This finding was also confirmed in the preliminary studies of the current research. Therefore, after demolding, mortar cubes containing PC were cured in water while the other samples were cured at room temperature at a relative humidity of over 80% until the test age. The use of different curing methods for $C\bar{S}A$ and PC-based blends allows for a comparison of $C\bar{S}A$ and PC performance, as it maximizes the performance of each. 0.5% (by mass of cement) citric acid monohydrate was used in mortars containing $C\bar{S}A$ to prevent rapid setting [12].

The products of hydration were investigated using paste samples and XRD (Olympus BTX-II) with a scanning range between 5 and 55°2θ and a resolution of 0.25°2θ using 24 h-old and 28 day-old specimens. Paste samples were prepared by mixing 50 g binder ($C\bar{S}A$ -Control, PC-LC^3-52, or $C\bar{S}A$ -LC^3-57) with deionized water at W/B = 0.40 and stirring manually for 2 min. The heat evolution of the mixtures was also measured, using an isothermal calorimeter (TAM Air) at 25 °C for 48 h. Scanning electron microscopy analysis (SEM) (Thermo Fisher Quanta 400F) was used to assess the microstructures of the hydrated pastes.

5 Discussion of Results

5.1 Influence of Mixture Proportions on Strength

Figure 3 shows the development of compressive strength of the mortars. $C\bar{S}A$ -Control has the highest 1-d strength, followed by PC-Control since these cements contain high proportions of clinker. All three $C\bar{S}A$ -LC^3 mortars gain greater strength than PC-LC^3-52 in this period and ~ 60–80% of that of PC-Control. The effectiveness of CSA in increasing early strength is evident since the clinker content of these $C\bar{S}A$ -LC^3 cements is 48–60% of that of PC-Control. This is attributed to the rapid formation of an ettringite skeleton.

The strength of PC-LC^3-52 more than doubled from 1 to 3 days and from 3 to 28 days, while $C\bar{S}A$ -LC^3 mortars showed more modest increases, paralleling the moderate strength increase of CSA-Control in this period. Long-term strength development in both systems relies on the hydration of calcium silicates. $C_3S + C_2S$ in PC clinker is much higher than C_2S in $C\bar{S}A$ clinker, leading to a lower amount of calcium hydroxide in hydrating $C\bar{S}A$. The lower pH

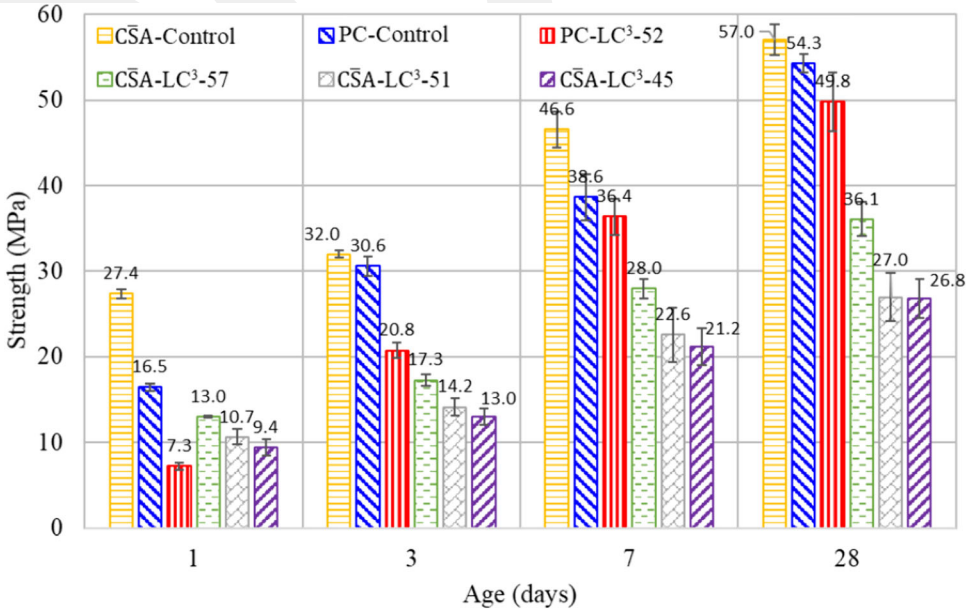

Fig. 3 Compressive strength development of the mixtures

Table 3 Flow table values of mixes

Mixtures	Flow (%)
C$\overline{S}$A -Control	110
PC-Control	110
PC-LC^3-52	70
C$\overline{S}$A -LC^3-57	85
C$\overline{S}$A -LC^3-51	80
C$\overline{S}$A -LC^3-45	85

likely decreased the dissolution of calcined clay in C$\overline{S}$A -LC^3 resulting in more limited strength gain and lower ultimate strengths than that of PC-LC^3-52. The strengths of C$\overline{S}$A -LC^3-45 and C$\overline{S}$A -LC^3-51 are close at all ages and nearly the same at 28 d while that of C$\overline{S}$A -LC^3-57 is significantly higher, by ~ 38%. This suggests that a threshold clinker content may be exceeded between 51 and 57% (for the particular clinker, clay, and limestone combination used here) similar to the ~ 50% value for typical LC^3 [5].

Table 3 presents a comparison of the flow of various mortars. The incorporation of calcined clay into PC reduces flow in PC-LC^3-52 compared with PC-Control. The layered structure and high specific surface area of calcined clay increase water demand [27, 45]. The flow of C$\overline{S}$A -LC^3 is slightly higher than that of PC-LC^3-52 since the calcined clay content is increased from 20 to 30%. Similar results were also reported by [20, 46]. Calcined clay dissolves partially or completely in an alkaline environment [47] but C$\overline{S}$A cement has a lower pH than PC. Thus, water demand in all C$\overline{S}$A -LC^3 is almost the same, regardless of calcined clay content.

5.2 Comparative Analysis of Strength and CO_2 Emissions

Despite its early and late strengths being lower than the PC control, the clinker content hence CO_2 footprint of C$\overline{S}$A -LC^3-57 is so much lower that it may be preferable when both technical and environmental performance are considered. Figure 4 shows strength gained per unit emission of CO_2, calculated by normalizing strengths at each age in Fig. 3 with the CO_2 footprints in Fig. 2.

As expected, despite gaining high strength, PC-Control has the lowest strength per CO_2 emission beyond 1 day due to its high carbon footprint. PC-LC^3-52 shows similar behavior up to 3 days, due to its slow initial strength gain. Among all the ternary mixes, C$\overline{S}$A -LC^3-57 has the highest strength per CO_2 emission at all ages, closest to that of C$\overline{S}$A -Control. C$\overline{S}$A -Control appears advantageous based on strength and carbon footprint considerations, however, the cost of C$\overline{S}$A -LC^3-57 or C$\overline{S}$A -LC^3-51 could be significantly lower, due to the reduced amount of C$\overline{S}$A clinker.

5.3 Influence of Mixture Proportions on Hydration Products

Figure 5 shows the microstructure of 1 day and 28 day old hydrated pastes of C$\overline{S}$A -Control, C$\overline{S}$A -LC^3-57, and PC-LC^3-52, selected since these mixes had higher strength per CO_2 performance than the others. The needle-shaped structures in the 1-day-old pastes are ascribed to ettringite. The formation of ettringite is responsible for a rapid decrease in porosity which leads to an increase in early strength and rapid setting [48]. The microstructure of PC-LC^3-52 changes with time, and the matrix consists of

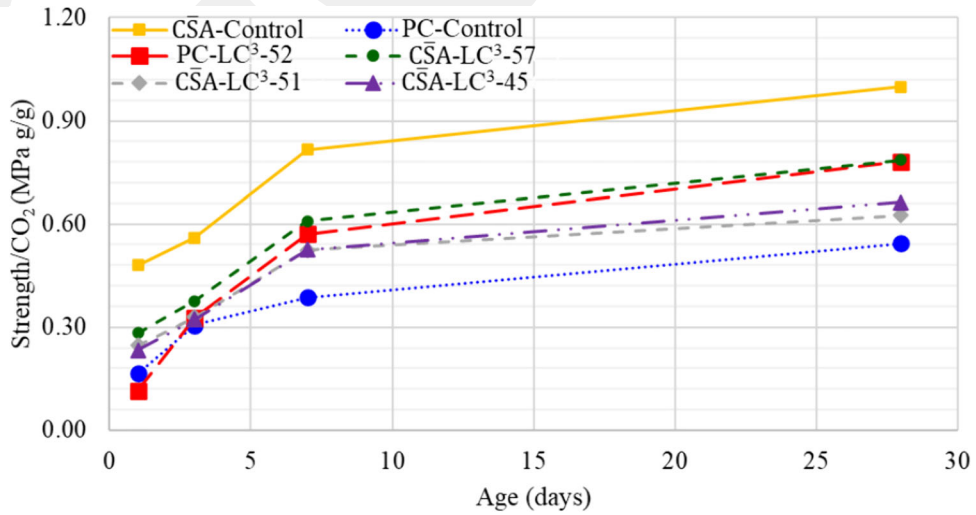

Fig. 4 Strength per CO_2 emission for the mixtures

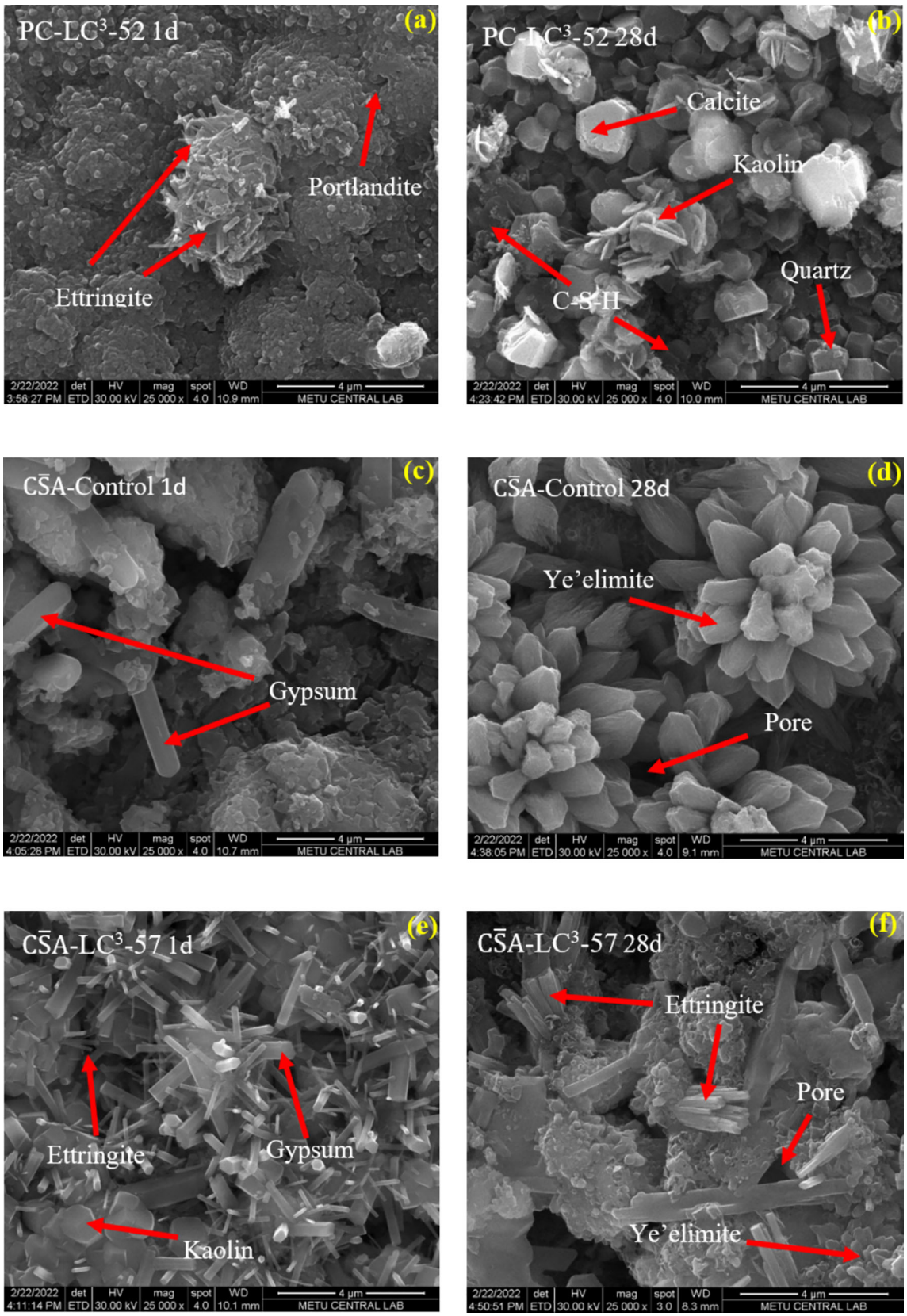

Fig. 5 1-day and 28-day SEM micrographs of: (a,b) PC-LC^3-52, (c,d) C$\bar{S}$A -Control, (e,f) C$\bar{S}$A -LC.^{3}-57

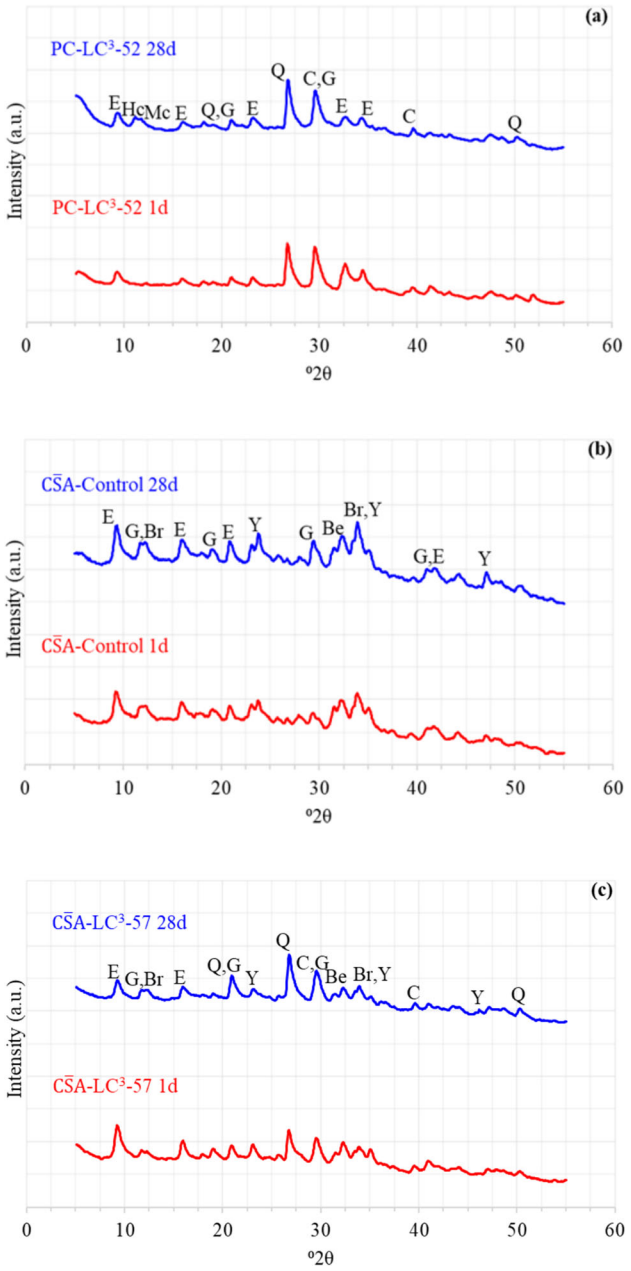

Fig. 6 X-ray diffractograms for (a) PC-LC^3-52 (b) CS̄A -Control (c) CS̄A -LC.^{3}-57 (Legend: E-ettringite; Hc-hemicarbonate; Mc-monocarbonate; Q-Quartz; G-Gypsum; C-Calcite; Br-Brownmillerite; Be-Belite; Y-Ye'elimite)

quartz, calcite, C-S–H, and kaolin particles with their typical layered structure [49–51]. Rhombic dodecahedron particles of unreacted ye'elimite were identified in CS̄A -Control and CS̄A -LC^3-57 at 28 days.

XRD analysis (Fig. 6) corroborates the observations in the micrographs. The main crystalline phases in PC-LC^3-52 are identified as ettringite, hemicarbonate, monocarbonate, quartz, gypsum, and calcite (Fig. 6a). Hemicarbonate and monocarbonate were absent at 1 day but exist at 28 days. The absence of these 2 products at early ages may be explained by the lack of sufficient amounts of portlandite, a hydration product of PC. The aluminate phase from PC reacts with calcium carbonate from limestone to form these two products at later ages. CS̄A -Control and CS̄A -LC^3-57 contain ettringite, gypsum, brownmillerite, belite and ye'elimite.

Although thermodynamic calculations in [23] predicted monocarbonate hydrate as a hydration product for a mixture of CS̄A cement with 10% metakaolin and 10%

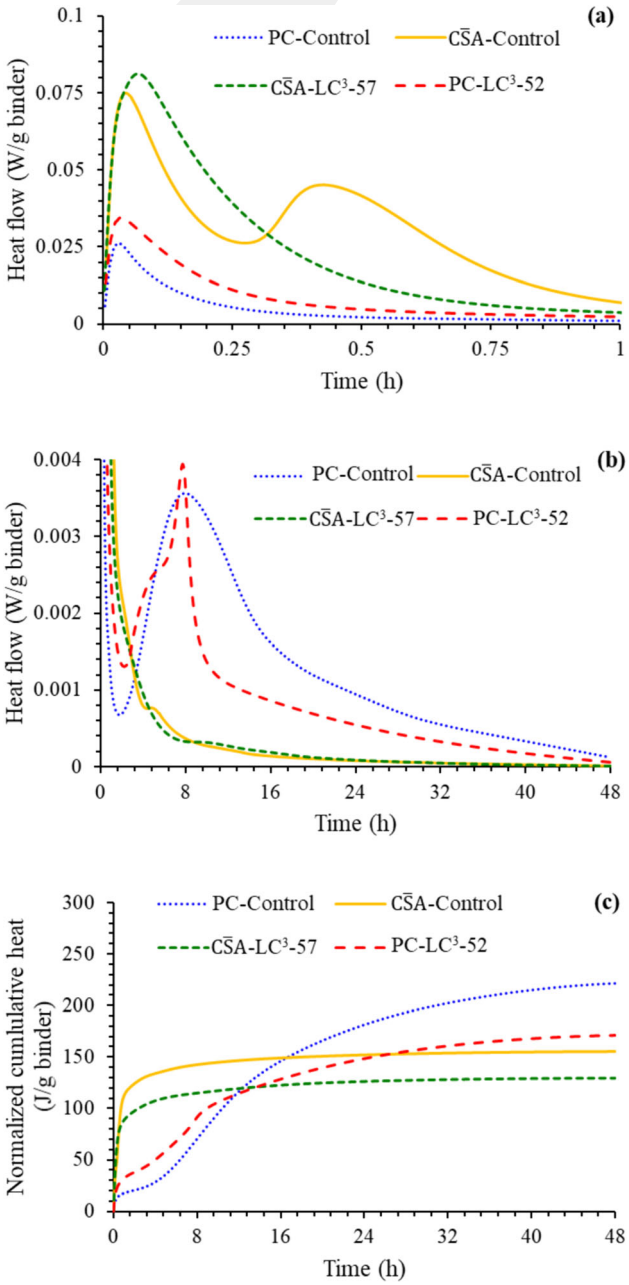

Fig. 7 Rate of heat evolution (a) in the first hour, (b) up to 48 h, and (c) cumulative heat evolved, for pastes hydrated at 25 °C

limestone, none was detected in $C\overline{S}A$ -LC^3-57. This may be due to the lack of calcium hydroxide and tricalcium aluminate in the system. Also, the clinker composition of $C\overline{S}A$ cement used in that study (62.7% ye'elimite, 10.7% belite, 8.2% fluorellestadite, and 5.7% bredigite) is very different from the $C\overline{S}A$ cement used in this study. In $C\overline{S}A$ -Control, the ettringite peaks grew with time due likely to the partial conversion of gypsum to ettringite. However, for $C\overline{S}A$ -LC^3-57, a clear decrease in the amount of ettringite was observed, and unreacted gypsum was still available at later ages. Ettringite formation at later ages may be due to the formation of amorphous aluminum hydroxide (AH_3). AH_3 precipitates inside pores in the paste and increases its compactness reducing the dissolution of anhydrous phases [52].

5.4 Influence of Mixture Proportions on Heat Evolution of Pastes

The rate of heat evolution and cumulative heat evolution are shown in Fig. 7 for various paste mixtures. During the preinduction period (Fig. 7a), the presence of calcined clay/limestone in both PC-Control and $C\overline{S}A$ -Control pastes accelerates hydration due to the filler effect [53]. Also, the rate of heat evolution in this period is significantly lower for PC-Control and PC-LC^3-52 than for mixtures containing $C\overline{S}A$ cement. The first peak in all pastes within the preinduction period was probably due to the dissolution and wetting of the pastes. The second peak, which occurs around 0.3– 0.6 h, in $C\overline{S}A$ -Control corresponds to ye'elimite and calcium sulfate dissolution with ettringite formation [54]. The third hydration peak was observed after a stagnant period which takes place due to the precipitation of ettringite formation on the surface of cement particles, lasting for 4.5 h. During this period, the reactions take place slowly. Eventually, the unhydrated cement particles react with water and hydration accelerates once again [55]. On the other hand, the rate of heat evolution for $C\overline{S}A$ -LC^3-57 gradually decreased after $\sim$ 10 min. Afterward, hydration is stagnant up to $\sim$ 9 h when a minor peak is observed. No additional hydration peaks are observed. The preinduction stage was followed by the induction period, acceleration period, and deceleration period as shown in Fig. 7b. In PC-Control and PC-LC^3-52, the second hydration peak occurs at $\sim$ 8 h. In addition, the PC-LC^3-52 paste exhibited a higher heat evolution rate and a narrow hydration peak, which can be attributed to the sulfate depletion caused by the aluminate reaction. $C\overline{S}A$ -LC^3-57 gives the lowest cumulative heat up to 48 h, while PC-Control gives the highest. At early ages (< 16 h), $C\overline{S}A$ -Control showed higher heat release, consistent with its higher 1-day strength. However, there is a crossover at about 16 h, and subsequently, PC-Control releases greater heat. The presence of calcined clay and limestone, on the other hand, decelerated the hydration of PC substantially.

Figure 8 illustrates the strong relationship between the cumulative heat hydration and strength at 1 day and 2 days. Whether LC^3 or control, mixtures containing the same clinker have the same particular strength-heat relationship, with the slope for $C\overline{S}A$ -containing mixtures much steeper than that of their PC-containing counterparts, due to their more crystalline nature. Hence, although not long-lasting, strength development is more efficient in $C\overline{S}A$ -LC^3 than in PC-LC^3. In both systems, the incorporation of calcined clay and limestone mostly has a dilution effect.

5.5 Cost analysis

Although Fig. 4 suggests that $C\overline{S}A$ cement is preferable based on strength and carbon footprint considerations, Fig. 9 shows that the cost of $C\overline{S}A$ -LC^3-57 or $C\overline{S}A$ -LC^3-51 is significantly lower than that of $C\overline{S}A$ -Control, due mainly to the reduced amount of $C\overline{S}A$ clinker. The calculations consider the transportation, grinding, and calcination of the materials (Table 4).

$C\overline{S}A$ -LC^3-57 costs $\sim$ 31% less to produce than $C\overline{S}A$ -Control, while only $\sim$ 16% more than PC-LC^3-52. The production costs of PC and $C\overline{S}A$ cement clinker are calculated as $\sim$ 60 USD/t and 62 USD/t, respectively, with the cost estimation for $C\overline{S}A$ cement clinker considering its ye'elimite content as in [56]. The $C\overline{S}A$ clinker used in this study contains $\sim$ 30% ye'elimite so its production cost is nearly equivalent to that of PC clinker.

Regarding transportation costs, it was assumed in [56] that gypsum, limestone, and calcined clay are sourced from locations $\sim$ 80 km away. Considering an electricity rate of 0.146 USD/kWh for grinding and including the calcination cost for clay, assumed to have undergone flash calcination, the data from Table 4 was used to calculate the costs of PC-LC^3 and $C\overline{S}A$ -LC^3 blends in Fig. 9. While the values in Fig. 9 may change for different assumptions, it is clear that replacing PC clinker in LC^3 with $C\overline{S}A$ clinker does not increase cost exorbitantly.

6 Conclusion

This study investigated the production of LC^3 incorporating $C\overline{S}A$ clinker instead of PC clinker. The following conclusions were drawn:

- LC^3 incorporating $C\overline{S}A$ has higher 1-d strength than typical LC^3 owing to the rapid hydration of $C\overline{S}A$.

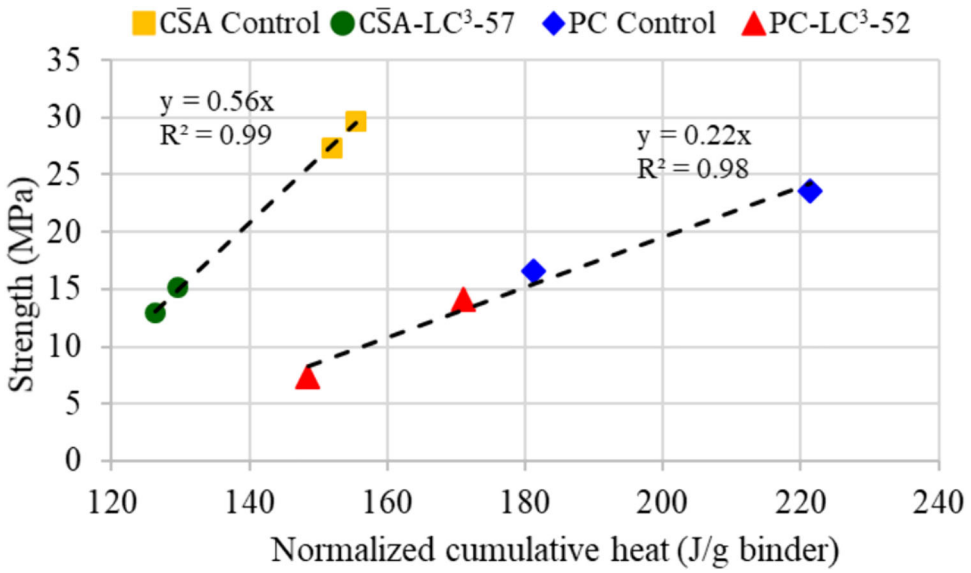

Fig. 8 Strength vs. normalized cumulative heat for mortars at 1 day and 2 days

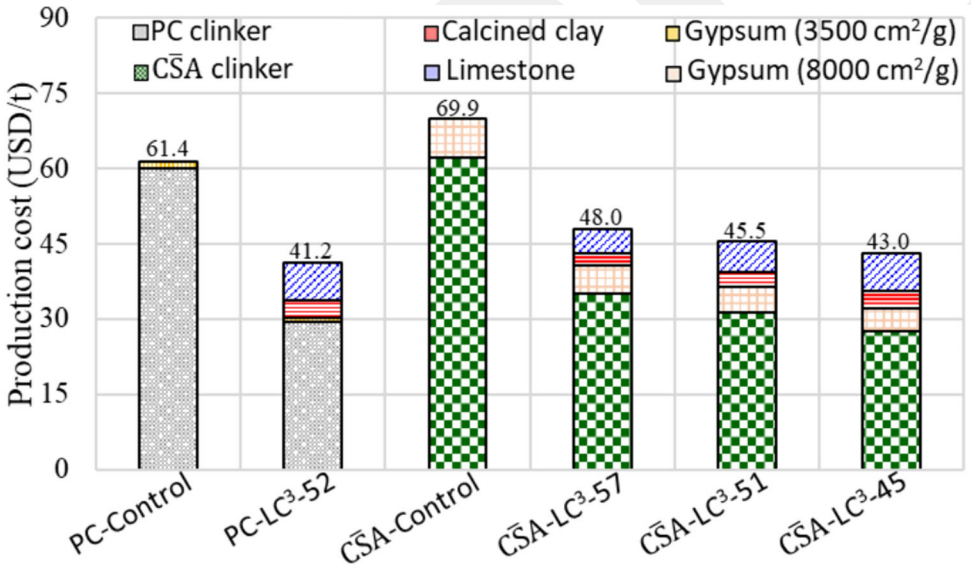

Fig. 9 Production cost of the binders studied

Beyond 1 day, strength is lower, as the calcined clay participates less in hydration reactions due to the lower alkalinity of the system.

- The CO_2 footprint of C$\bar{S}$A -LC^3 is lower than that of PC-LC^3, at similar clinker contents. Consequently, strength gained per unit CO_2 emission is similar for C$\bar{S}$A -LC^3 and PC-LC^3. The inclusion of calcined clay and limestone into C$\bar{S}$A also reduces the cost of this cement type.
- The primary hydration product formed in C$\bar{S}$A -LC^3 is ettringite. Gypsum, brownmillerite, ye'elimite, quartz, and calcite are also present, at both early and later ages. Hemicarbonate and monocarbonate phases are not identified, possibly due to the absence of portlandite and C_3A.
- C$\bar{S}$A -LC^3 generates significantly less heat than PC-LC^3, PC-Control, and C$\bar{S}$A -Control, ultimately.
- The production cost of C$\bar{S}$A -LC^3 mixtures is estimated to be notably lower than that of C$\bar{S}$A -Control and only slightly higher than PC-LC^3. Hence, they may find use in construction applications where the carbon footprint needs to be lowered while maintaining adequate early-age strength.

Table 4 Cost and energy consumption data related to the processing of raw materials [35, 56, 57]

Process	Limestone	Raw clay	Gypsum (3500 cm^2/g)	Gypsum (8000 cm^2/g)
Transportation and procurement cost (USD/t)	3.5	6.1	22	22
Energy consumption for grinding, kWh (grinding time, h)	103.5 (6)	82.0 (4)	8.9 (0.5)	103.4 (6)
Grinding cost (USD/t)	15.1	12.0	1.3	15.1
Calcination (USD/t)	–	6.92	–	–

Author Contributions All authors contributed to the study conception and design. Material preparation, data collection and analysis were performed by [MA] and [STE]. The first draft of the manuscript was written by [STE] and all authors commented on previous versions of the manuscript. All authors read and approved the final manuscript.

Funding The authors did not receive support from any organization for the submitted work.

Data availability Datasets generated during and/or analysed during this study are available from the corresponding author on reasonable request.

Declarations

Conflict of Interest The authors declare that they have no known competing financial interests or personal relationships that could have appeared to influence the work reported in this paper. No potential conflict of interest was reported by the authors.

References

1. Wang T, Gao X (2018) Reflection and operationalization of the common but differentiated responsibilities and respective capabilities principle in the transparency framework under the international climate change regime. Adv Clim Chang Res 9(4):253–263. https://doi.org/10.1016/j.accre.2018.12.004
2. Rogelj J, Popp A, Calvin KV, Luderer G, Emmerling J, Gernaat D, Fujimori S, Strefler J, Hasegawa T, Marangoni G, Krey V, Kriegler E, Riahi K, Vuuren DPV, Doelman J, Drouet L, Edmonds J, Fricko O, Harmsen M, Havlík P, Humpenöder F, Stehfest E, Tavoni M (2018) Scenarios towards limiting global mean temperature increase below 15°C. Nat Clim Change 8(4):325–332. https://doi.org/10.1038/s41558-018-0091-3
3. Hasanbeigi A, Price L, Lu H, Lan W (2010) Analysis of energy-efficiency opportunities for the cement industry in Shandong Province, China: a case study of 16 cement plants. Energy 35(8):3461–3473. https://doi.org/10.1016/j.energy.2010.04.046
4. Kumar Das S, Adediran A, Rodrigue Kaze C, Mohammed Mustakim S, Leklou N (2022) Production, characteristics, and utilization of rice husk ash in alkali activated materials: an overview of fresh and hardened state properties. Constr Build Mater 345:128341. https://doi.org/10.1016/j.conbuildmat.2022.128341
5. Antoni M, Rossen J, Martirena F, Scrivener K (2012) Cement substitution by a combination of metakaolin and limestone. Cem Concr Res 42(12):1579–1589. https://doi.org/10.1016/J.CEMCONRES.2012.09.006
6. Maraghechi H, Avet F, Wong H, Kamyab H, Scrivener K (2018) Performance of limestone calcined clay cement (LC3) with various kaolinite contents with respect to chloride transport. Mater Struct 51(5):125. https://doi.org/10.1617/s11527-018-1255-3
7. Huang Z, Huang Y, Liao W, Han N, Zhou Y, Xing F, Sui T, Wang B, Ma H (2020) Development of limestone calcined clay cement concrete in South China and its bond behavior with steel reinforcement. J Zhejiang Univ-Sci A 21(11):892–907. https://doi.org/10.1631/jzus.A2000163
8. De Weerdt K, Haha MB, Le Saout G, Kjellsen KO, Justnes H, Lothenbach B (2011) Hydration mechanisms of ternary Portland cements containing limestone powder and fly ash. Cem Concr Res 41(3):279–291. https://doi.org/10.1016/j.cemconres.2010.11.014
9. Hay R, Li L, Celik K (2022) Shrinkage, hydration, and strength development of limestone calcined clay cement (LC3) with different sulfation levels. Cement Concr Compos 127:104403. https://doi.org/10.1016/j.cemconcomp.2021.104403
10. Hanein T, Galvez-Martos JL, Bannerman MN (2018) Carbon footprint of calcium sulfoaluminate clinker production. J Clean Prod 172:2278–2287. https://doi.org/10.1016/j.jclepro.2017.11.183
11. Sharp JH, Lawrence CD, Yang R (1999) Calcium sulfoaluminate cements—low-energy cements, special cements or what? Adv Cem Res 11(1):3–13. https://doi.org/10.1680/adcr.1999.11.1.3
12. Canbek O, Erdoğan ST (2020) Influence of production parameters on calcium sulfoaluminate cements. Constr Build Mater 239:117866. https://doi.org/10.1016/j.conbuildmat.2019.117866
13. Beretka J, De Vito B, Santoro L, Sherman N, Valenti GL (1993) Hydraulic behaviour of calcium sulfoaluminate-based cements derived from industrial process wastes. Cem Concr Res 23(5):1205–1214. https://doi.org/10.1016/0008-8846(93)90181-8
14. Luz C, Rocha J, Cheriaf M, Pera J (2006) Use of sulfoaluminate cement and bottom ash in the solidification/stabilization of galvanic sludge. J Hazard Mater 136(3):837–845. https://doi.org/10.1016/j.jhazmat.2006.01.020
15. Pace ML, Telesca A, Marroccoli M, Valenti GL (2011) Use of industrial byproducts as alumina sources for the synthesis of calcium sulfoaluminate cements. Environ Sci Technol 45(14):6124–6128. https://doi.org/10.1021/es2005144
16. Martin LHJ, Winnefeld F, Müller CJ, Lothenbach B (2015) Contribution of limestone to the hydration of calcium sulfoaluminate cement. Cement Concr Compos 62:204–211. https://doi.org/10.1016/j.cemconcomp.2015.07.005
17. Canbek O, Shakouri S, Erdoğan ST (2020) Laboratory production of calcium sulfoaluminate cements with high industrial waste content. Cement Concr Compos 106:103475. https://doi.org/10.1016/j.cemconcomp.2019.103475
18. Yoon HN, Seo J, Kim S, Lee HK, Park S (2021) Hydration of calcium sulfoaluminate cement blended with blast-furnace slag. Constr Build Mater 268:121214. https://doi.org/10.1016/j.conbuildmat.2020.121214
19. Li J, Ma B, Zhou C, Yang Y (2014) Study on mechanism of chemical activation for minerals of high belite-calcium

sulfoaluminate clinker. J Sustain Cement-Based Mater 3(1):13–23. https://doi.org/10.1080/21650373.2013.843476
20. Zhou Y, Wang Z, Zhu Z, Chen Y, Wu K, Huang H, Anvarovna KG, Xu L (2022) Influence of metakaolin and calcined montmorillonite on the hydration of calcium sulphoaluminate cement. Case Stud Construct Mater 16:e01104. https://doi.org/10.1016/j.cscm.2022.e01104
21. Gao D, Meng Y, Yang L, Tang J, Lv M (2019) Effect of ground granulated blast furnace slag on the properties of calcium sulfoaluminate cement. Constr Build Mater 227:116665. https://doi.org/10.1016/j.conbuildmat.2019.08.046
22. Xu J, Chen J, Lu D, Xu Z, Hooton RD (2019) Effect of dolomite powder on the hydration and properties of calcium sulfoaluminate cements with different gypsum contents. Constr Build Mater 225:302–310. https://doi.org/10.1016/j.conbuildmat.2019.07.050
23. Pedersen M, Lothenbach B, Winnefeld F, Skibsted J (2018) Hydrate Phase Assemblages in Calcium Sulfoaluminate – Metakaolin – Limestone Blends. In: Martirena F, Favier A, Scrivener K (eds) Calcined Clays for Sustainable Concrete. Springer, Netherlands, Dordrecht
24. Essolebe E A 2023 Low embodied CO2 Binders using Belitic Calcium Sulfoaluminate Cement. Master's Thesis, University of California, Los Angeles, United States.
25. ASTM C618–22 (2023) Standard specification for coal fly ash and raw or calcined natural pozzolan for use in concrete, Annual Book of ASTM standards, ASTM International, West Conshohocken, PA
26. ASTM C563–20 (2020) Standard guide for approximation of optimum so3 in hydraulic cement, Annual Book of ASTM standards, ASTM International, West Conshohocken, PA
27. Muzenda TR, Hou P, Kawashima S, Sui T, Cheng X (2020) The role of limestone and calcined clay on the rheological properties of LC3. Cement Concr Compos 107:103516. https://doi.org/10.1016/j.cemconcomp.2020.103516
28. Rodriguez C, Tobon JI (2020) Influence of calcined clay/limestone, sulfate and clinker proportions on cement performance. Constr Build Mater 251:119050. https://doi.org/10.1016/j.conbuildmat.2020.119050
29. Cardinaud G, Rozière E, Martinage O, Loukili A, Barnes-Davin L, Paris M, Deneele D (2021) Calcined clay – Limestone cements: hydration processes with high and low-grade kaolinite clays. Constr Build Mater 277:122271. https://doi.org/10.1016/j.conbuildmat.2021.122271
30. Rengaraju S, Pillai RG (2023) Long-term corrosion performance and monitoring for service life estimation of LC3 concrete systems. J of Sustain Cement-Based Mater 12(12):1592–1603. https://doi.org/10.1080/21650373.2023.2246068
31. Scrivener K, Martirena F, Bishnoi S, Maity S (2018) Calcined clay limestone cements (LC3). Cem Concr Res 114:49–56. https://doi.org/10.1016/j.cemconres.2017.08.017
32. Krishnan S, Bishnoi S (2018) Understanding the hydration of dolomite in cementitious systems with reactive aluminosilicates such as calcined clay. Cem Concr Res 108:116–128. https://doi.org/10.1016/j.cemconres.2018.03.010
33. Bernal IMR, Aranda MAG, Santacruz I, De La Torre AG, Cuesta A (2023) Early-age reactivity of calcined kaolinitic clays in LC3 cements: a multitechnique investigation including pair distribution function analysis. J Sustain Cement-Based Mater 12(6):721–735. https://doi.org/10.1080/21650373.2022.2117248
34. Avet F, Li X, Scrivener K (2018) Determination of the amount of reacted metakaolin in calcined clay blends. Cem Concr Res 106:40–48. https://doi.org/10.1016/j.cemconres.2018.01.009
35. Tokyay M (2016) Cement and Concrete Mineral Admixtures. CRC Press, Boca Raton
36. Khaled Z, Mohsen A, Soltan A, Kohail M (2023) Optimization of kaolin into metakaolin: calcination conditions, mix design and curing temperature to develop alkali activated binder. Ain Shams Eng J. https://doi.org/10.1016/j.asej.2023.102142
37. Murat M, Comel C (1983) Hydration reaction and hardening of calcined clays and related minerals III. influence of calcination process of kaolinite on mechanical strengths of hardened metakaolinite. Cem Con Res 13(5):631–637. https://doi.org/10.1016/0008-8846(83)90052-2
38. He C, Osbaeck B, Makovicky E (1995) Pozzolanic reactions of six principal clay minerals: activation, reactivity assessments and technological effects. Cem Concr Res 25(8):1691–1702. https://doi.org/10.1016/0008-8846(95)00165-4
39. Choate WT (2003) Energy and emission reduction opportunities for the cement industry. Columbia (United States). https://doi.org/10.2172/1218753
40. Hanein T, Thienel KC, Zunino F, Marsh ATM, Maier M, Wang B, Canut M, Juenger MCG, Ben Haha M, Avet F, Parashar A, Al-Jaberi LA, Almenares-Reyes RS, Alujas-Diaz A, Scrivener K, Bernal SA, Provis JL, Sui T, Bishnoi S, Martirena-Hernández F (2022) Clay calcination technology: state-of-the-art review by the RILEM TC 282-CCL. Mater Struct 55:1–3. https://doi.org/10.1617/s11527-021-01807-6
41. ASTM C305–20 (2020) Standard practice for mechanical mixing of hydraulic cement pastes and mortars of plastic consistency, Annual Book of ASTM standards, ASTM International, West Conshohocken, PA
42. ASTM C109/109M (2021) Standard test method for compressive strength of hydraulic cement mortars (Using 2-in. or cube specimens), Annual Book of ASTM standards, ASTM International, West Conshohocken, PA
43. ASTM C1437–20 (2020) Standard test method for flow of hydraulic cement mortar, Annual Book of ASTM standards, ASTM International, West Conshohocken, PA
44. Li N, Xu L, Wang R, Li L, Wang P (2018) Experimental study of calcium sulfoaluminate cement-based self-leveling compound exposed to various temperatures and moisture conditions: hydration mechanism and mortar properties. Cem Concr Res 108:103–115. https://doi.org/10.1016/j.cemconres.2018.03.012
45. Ferreiro S, Herfort D, Damtoft JS (2017) Effect of raw clay type, fineness, water-to-cement ratio and fly ash addition on workability and strength performance of calcined clay – limestone Portland cements. Cem Concr Res 101:1–12. https://doi.org/10.1016/j.cemconres.2017.08.003
46. Khaleel OR, Razak HA (2012) The effect of powder type on the setting time and self compactability of mortar. Constr Build Mater 36:20–26. https://doi.org/10.1016/j.conbuildmat.2012.04.079
47. Zunino F, Dhandapani Y, Ben Haha M, Skibsted J, Joseph S, Krishnan S, Parashar A, Juenger MCG, Hanein T, Bernal SA, Scrivener K, Avet F (2022) Hydration and mixture design of calcined clay blended cements: review by the RILEM TC 282-CCL. Mater Struct 55(9):234. https://doi.org/10.1617/s11527-022-02060-1
48. Chen W, Ling X, Li Q, Yuan B, Li B, Ma H (2019) Experimental evidence on formation of ulexite in sulfoaluminate cement paste mixed with high concentration borate solution and its retarding effects. Constr Build Mater 215:777–785. https://doi.org/10.1016/j.conbuildmat.2019.04.242
49. Li J, Wang X, Wu W (2021) Quantification of SEM quartz grain identifying the depositional environment. Arab J Geosci 14(11):1006. https://doi.org/10.1007/s12517-021-07442-3
50. Vergara LA, Colorado HA (2020) Additive manufacturing of Portland cement pastes with additions of kaolin, superplastificant and calcium carbonate. Constr Build Mater 248:118669. https://doi.org/10.1016/j.conbuildmat.2020.118669
51. Sui H, Hou P, Liu Y, Sagoe-Crentsil K, Basquiroto de Souza F, Duan W (2023) Limestone calcined clay cement: mechanical

properties, crystallography, and microstructure development. J Sustain Cement-Based Mater 12(4):427–440. https://doi.org/10.1080/21650373.2022.2074911
52. Chang J, Zhang Y, Shang X, Zhao J, Yu X (2017) Effects of amorphous AH3 phase on mechanical properties and hydration process of C4A3S-CSH2-CH-H2O system. Constr Build Mater 133:314–322. https://doi.org/10.1016/j.conbuildmat.2016.11.111
53. Zunino F, Scrivener K (2019) The influence of the filler effect on the sulfate requirement of blended cements. Cem Concr Res 126:105918. https://doi.org/10.1016/j.cemconres.2019.105918
54. Bolaños-Vásquez I, Trauchessec R, Tobón JI, Lecomte A (2020) Influence of the ye'elimite/anhydrite ratio on PC-CSA hybrid cements. Mater Today Commun 22:100778. https://doi.org/10.1016/j.mtcomm.2019.100778
55. Li J, Wang R, Xu Y (2022) Influence of cellulose ethers chemistry and substitution degree on the setting and early-stage hydration of calcium sulphoaluminate cement. Constr Build Mater 344:128266. https://doi.org/10.1016/j.conbuildmat.2022.128266
56. Gálvez-Martos JL, Chaliulina R, Elhoweris A, Mwanda J, Hakki A, Al-Horr Y (2021) Techno-economic assessment of calcium sulfoaluminate clinker production using elemental sulfur as raw material. J Clean Prod 301:126888. https://doi.org/10.1016/j.jclepro.2021.126888
57. Panesar DK, Kanraj D, Abualrous Y (2019) Effect of transportation of fly ash: Life cycle assessment and life cycle cost analysis of concrete. Cement Concr Compos 99:214–224. https://doi.org/10.1016/j.cemconcomp.2019.03.019